



## The Effects of Artificial Selection on the Maize Genome

Stephen I. Wright, *et al.*  
*Science* **308**, 1310 (2005);  
DOI: 10.1126/science.1107891

**The following resources related to this article are available online at [www.sciencemag.org](http://www.sciencemag.org) (this information is current as of August 6, 2007):**

A correction has been published for this article at:  
<http://www.sciencemag.org/cgi/content/full/310/5745/54>

**Updated information and services**, including high-resolution figures, can be found in the online version of this article at:  
<http://www.sciencemag.org/cgi/content/full/308/5726/1310>

**Supporting Online Material** can be found at:  
<http://www.sciencemag.org/cgi/content/full/308/5726/1310/DC1>

A list of selected additional articles on the Science Web sites **related to this article** can be found at:

<http://www.sciencemag.org/cgi/content/full/308/5726/1310#related-content>

This article **cites 25 articles**, 18 of which can be accessed for free:  
<http://www.sciencemag.org/cgi/content/full/308/5726/1310#otherarticles>

This article has been **cited by** 59 article(s) on the ISI Web of Science.

This article has been **cited by** 36 articles hosted by HighWire Press; see:  
<http://www.sciencemag.org/cgi/content/full/308/5726/1310#otherarticles>

This article appears in the following **subject collections**:  
Evolution  
<http://www.sciencemag.org/cgi/collection/evolution>

Information about obtaining **reprints** of this article or about obtaining **permission to reproduce this article** in whole or in part can be found at:  
<http://www.sciencemag.org/about/permissions.dtl>

Fig. 1), both of which close their leaves rapidly to capture prey; *Aldrovanda* closes its leaves in  $\sim 0.02$  s, whereas the Venus flytrap closes in  $\sim 0.2$  s. However, although the leaves of the Venus flytrap snap by reversing their curvature, *Aldrovanda*'s leaves are already initially curved inward so that closure does not produce a snap. To understand how the snapless *Aldrovanda* can be more rapid than the snapping Venus flytrap, we use Eq. (1) for the poroelastic time: for a Venus flytrap leaf of typical thickness  $L = 0.5$  mm,  $\tau_p = 1.6$  s/mm<sup>2</sup>  $(0.5 \text{ mm})^2 \sim 0.4$  s, whereas for an *Aldrovanda*  $L = 0.05$  mm, the value of  $\tau_p$  is  $\sim 0.004$  s. Because an *Aldrovanda* leaf is about 1/10th the size of the Venus flytrap, it can be actuated 100 times more rapidly and does not require an elastic instability to catch prey, whereas the Venus flytrap does, which is consistent with our classification.

The absolute physical limit of motion in self-actuated mechanical systems is determined by the speed of elastic waves in them, which propagate at a speed that scales as  $\sqrt{E/\rho}$ . This yields an estimate for the inertial time given by

$$\tau_i \sim L\sqrt{(\rho/E)} < \tau \quad (2)$$

The inertial time scale characterizes the time for wave propagation in mechanical

signalling in systems and must be less than  $\tau$ , the time scale of the motion. In Fig. 1, the solid line denotes  $\tau_i/L \sim 10^{-5}$  s/mm, consistent with typical values for soft plant tissue (3, 11), beyond which there can be no natural nastic movements. For the fungus *Pilobolus*'s sporangium discharge (13),  $L \sim 0.05$  mm, so that  $\tau_i \sim 10^{-7}$  s  $< 10^{-5}$  s  $\sim \tau$ , whereas for fruit of *Hura crepitans* (2),  $L \sim 5$  mm, so that  $\tau_i \sim 10^{-5}$  s  $< 10^{-4}$  s  $\sim \tau$ , as shown in Fig. 1. These explosive movements characterize Nature's best attempts to reach the physical limits of autonomous motion in elastic tissues.

In conclusion, we see that the size-dependent inertial-elastic time  $\tau_i$  and the poroelastic time  $\tau_p$  given by Eqs. (1) and (2) provide us with a physical basis for the classification of the hydraulic movements in plants and fungi and yield limits on their performance. This implies that the engineering of soft, nonmuscular hydraulically actuated systems for rapid movement requires either small size or the enhancement of motion on large scales via elastic instabilities. Nature has already implemented many such designs exquisitely; we simply need to follow her lead.

#### References and Notes

1. D. Attenborough, *The Private Life of Plants* (BBC Books, London, 1995).
2. M. D. Swaine, T. Beer, *New Phytol.* **78**, 695 (1977).

3. Y. Forterre, J. M. Skotheim, J. Dumais, L. Mahadevan, *Nature* **433**, 421 (2005).
4. J. Comandon, P. de Fonbrune, *C.R. Soc. Biol. Paris* **129**, 620 (1938).
5. O. V. S. Heath, *New Phytol.* **37**, 385 (1938).
6. This is a reasonable first approximation when the pore size does not change much and when the fluid is Newtonian. Then, the fluid shear viscosity, which characterizes the resistance of the fluid to shear, is a constant. For a simple derivation of Darcy's law in the context of poroelasticity, see (9); for a discussion of its implications in confined geometries, see (10).
7. The pressure, which has the units of force per unit area, characterizes the local isotropic component of the stress.
8.  $E$  is the drained elastic bulk modulus of the tissue, which characterizes the response of the tissue when the fluid is equilibrated.  $u$  denotes the typical tissue displacement, i.e., the distance a point in the tissue has moved from its initial position. We have assumed that the material behaves linearly, i.e., that the elastic stress is proportional to the strain. This assumption is usually a good one because the typical strains involved are of the order of a few percent at most.
9. M. A. Biot, *J. Appl. Phys.* **12**, 155 (1941).
10. J. M. Skotheim, L. Mahadevan, *Proc. R. Soc. Lond. A Math. Phys. Eng.* **460**, 1995 (2004).
11. J. French, E. Steudle, *Plant Physiol.* **91**, 719 (1989).
12. J. Ashida, *Mem. Coll. Sci. Kyoto Imp. Univ. B IX*, 141 (1934).
13. R. M. Page, *Science* **146**, 925 (1964).

#### Supporting Online Material

www.sciencemag.org/cgi/content/full/308/5726/1308/DC1  
SOM Text  
Table S1

29 November 2004; accepted 15 March 2005  
10.1126/science.1107976

## The Effects of Artificial Selection on the Maize Genome

Stephen I. Wright,<sup>1,3</sup> Irie Vroh Bi,<sup>4\*</sup> Steve G. Schroeder,<sup>4</sup>  
Masanori Yamasaki,<sup>4</sup> John F. Doebley,<sup>5</sup> Michael D. McMullen,<sup>4,6</sup>  
Brandon S. Gaut<sup>1,2,†</sup>

Domestication promotes rapid phenotypic evolution through artificial selection. We investigated the genetic history by which the wild grass teosinte (*Zea mays* ssp. *parviglumis*) was domesticated into modern maize (*Z. mays* ssp. *mays*). Analysis of single-nucleotide polymorphisms in 774 genes indicates that 2 to 4% of these genes experienced artificial selection. The remaining genes retain evidence of a population bottleneck associated with domestication. Candidate selected genes with putative function in plant growth are clustered near quantitative trait loci that contribute to phenotypic differences between maize and teosinte. If we assume that our sample of genes is representative,  $\sim 1200$  genes throughout the maize genome have been affected by artificial selection.

Maize domestication has resulted in highly modified inflorescence and plant architecture (1). Improvement after domestication has also resulted in striking changes in yield, plant habit, biochemical composition, and other traits. At the genetic level, these phenotypic shifts are the result of strong directional (artificial) selection on target genes. With rare exceptions (2), targeted genes have not been identified.

Most domesticated plants and animals have experienced a "domestication bottleneck" that reduced genetic diversity relative to their wild ancestor (3). This bottleneck affects all genes

in the genome and modifies the distribution of genetic variation among loci. The magnitude and variance of the reduction in genetic diversity across loci provide insights into the demographic history of domestication. However, in genes targeted by artificial selection, genetic diversity is reduced above and beyond that caused by the domestication bottleneck (4). Selection is similar to a more severe bottleneck (5) that removes most (or all) of the genetic variation from a target locus.

Here, we report single-nucleotide polymorphism (SNP) diversity in 774 gene fragments

(100 to 900 base pairs) in a sample of 14 maize inbred lines (representing modern maize) and 16 inbred teosintes (tables S1 and S2). In this gene set, we have identified 3463 SNPs in maize and 6136 SNPs in teosinte. The polymorphism data are generally consistent with a population bottleneck during the domestication of maize.

Diversity, as measured by Watterson's estimator of the population mutation parameter  $\theta$  (6), is reduced in maize relative to teosinte (Fig. 1). Our maize sample has about 57% of the variability found in its progenitor. This is somewhat lower than previous estimates that were based on a smaller number of genes (7, 8). The difference in part reflects differences in sampling and the presence of several loci with no polymorphism in maize; 65 maize genes in our data set contain no segregating sites.

<sup>1</sup>Department of Ecology and Evolutionary Biology, <sup>2</sup>Institute of Genomics and Bioinformatics, University of California, Irvine, CA 92697, USA. <sup>3</sup>Department of Biology, York University, Toronto, Ontario M3J 1P3, Canada. <sup>4</sup>Department of Agronomy, Plant Science Unit, University of Missouri, Columbia, MO 65211, USA. <sup>5</sup>Department of Genetics, University of Wisconsin, Madison, WI 53706, USA. <sup>6</sup>Plant Genetics Research Unit, USDA-Agricultural Research Service, Columbia, MO 65211, USA.

\*Present address: Institute for Genomic Diversity, Cornell University, Ithaca, NY 14853, USA.

†To whom correspondence should be addressed. E-mail: bgaut@uci.edu

Linkage disequilibrium (LD) is increased in maize relative to teosinte. We have estimated the population recombination parameter  $\rho$  (9), which is inversely proportional to LD. The average estimate of  $\rho$  in maize is 17% that of teosinte (Fig. 1). Thus, estimates of  $\rho$  in maize have been reduced more drastically than estimates of  $\theta$ , as expected under a recent population bottleneck (10). The ratio  $\rho/\theta$ , the relative rate of recombination to mutation under the neutral equilibrium model, has declined sharply in maize relative to teosinte, from 4.5 in teosinte to 1.5 in maize. These results suggest that patterns of LD in maize are strongly influenced by population history, perhaps more so than by extant recombination rates.

Finally, the frequency distribution of polymorphisms, as measured by Tajima's  $D$ , has shifted between maize and teosinte (Fig. 1). In teosinte, polymorphisms are skewed toward rare variants, and the average  $D$  ( $\bar{D}$ ) across loci is  $-0.50$ . In contrast,  $\bar{D}$  is slightly positive (0.04) in maize, indicating a shift toward higher frequency alleles. This frequency shift is also expected after a recent bottleneck (11), because increased rates of genetic drift during a bottleneck tend to remove rare variants preferentially.

Our genome-wide estimates of SNP diversity from maize and teosinte provide a basis to estimate the demographic history of maize and to test for selection. We used coalescent simulations to infer the severity of the domestication bottleneck. Our coalescent model incorporates information about maize, such as the domestication time  $\sim 7500$  years ago (7, 12) and the inference of a single domestication event (13). The model also uses diversity data from teosinte to control for variation in stochastic effects, mutation rates, and recombination rates among loci. Our simulation method differs from previously published methods in the use of a rejection-sampling scheme, which fits simulated data to multiple summaries of the teosinte data. Our reasoning for the rejection-sampling approach is that the demographic history of teosinte is unknown but is reflected in sequence data. By conditioning simulated data on observed data, our simulations capture much of the historical features of each locus. In the rejection-sampling process, simulations that mimic teosinte data are retained, compared to maize data, and then interpreted in a likelihood framework for parameter estimation and model testing (14).

The primary parameter of interest is maize bottleneck severity ( $k$ ), which is the ratio of the size of the bottlenecked population ( $N_b$ ) to the duration of the bottleneck ( $d$ ) in generations. To estimate  $k$ , we simulated teosinte and maize data for each of 774 loci, varying bottleneck severity for different sets of simulations to find the best fitting model. The multilocus data are most consistent with a domestication bottleneck of moderate size, with  $\hat{k}$ , the maximum likelihood (ML) esti-

mate of  $k$ , equal to 2.45 (Fig. 2A). This estimate is slightly smaller than a previous estimate based on 12 loci (7), but the inference is robust to variation in model parameters such as domestication time, size of the predomestication population, and size of the current maize population (fig. S2). With independent information about  $d$ ,  $\hat{k}$  provides insight into the founding population of maize. For example, the archaeological record suggests that the

maximum estimate of  $d$  for the domestication of maize is  $\sim 2800$  years (12), assuming one generation per year for an annual plant. Under this time scale,  $N_b$  is 6860 chromosomes, which implies that fewer than 3500 individuals, or  $<10\%$  (15, 16) of the teosinte population, contributed to the genetic diversity captured in our maize sample.

How well do the observed data fit this simple bottleneck model? We generated a simu-

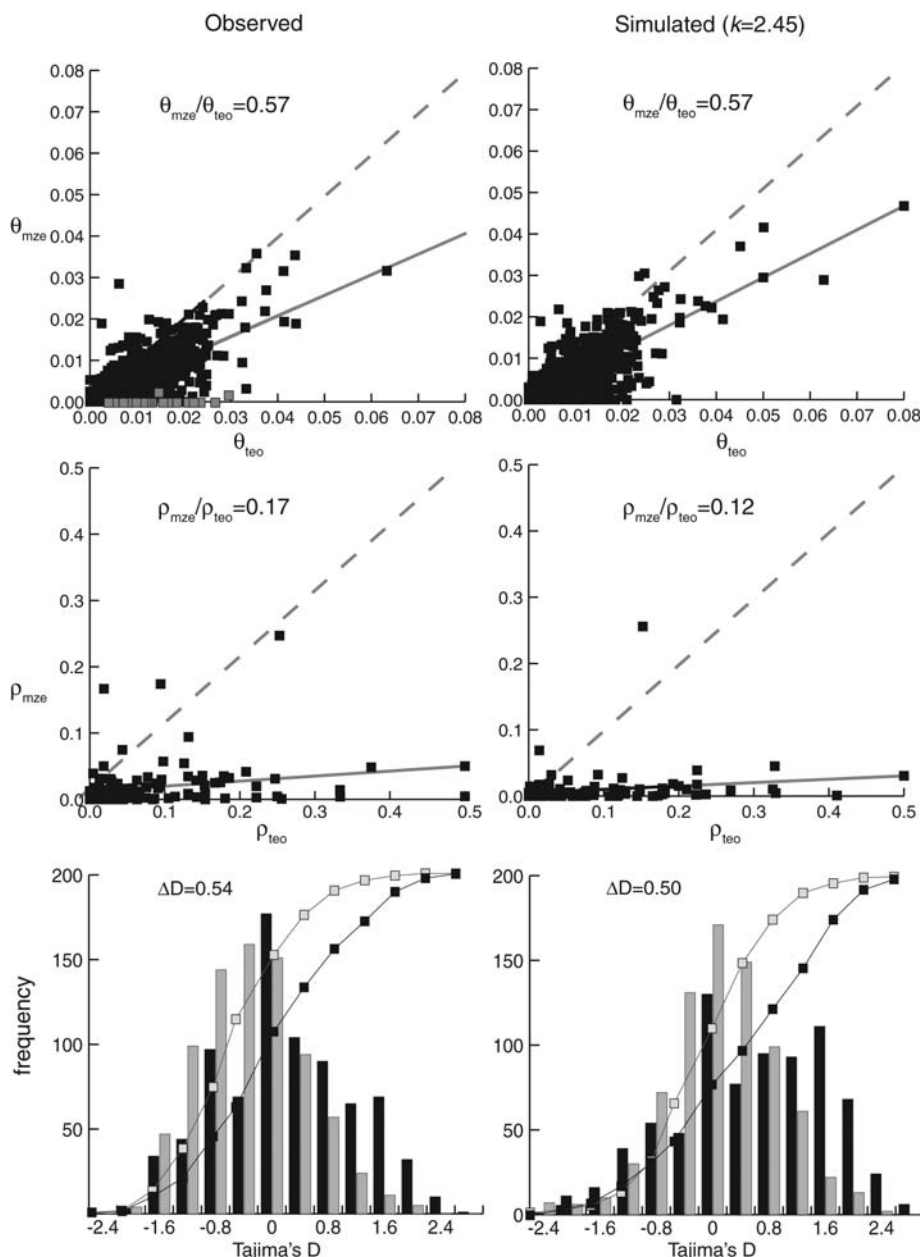


**Fig. 1.** Patterns of diversity in maize and teosinte at 774 gene fragments. The first column plots the observed data; the second column graphs a simulated data set with  $k = 2.45$  (14). The first row illustrates the relationship between mean values of  $\theta$  in teosinte (x axis) versus maize (y axis). Dashed diagonal lines have a slope of 1.0, representing equal diversity between taxa; solid lines are regression lines. Each square represents a single gene, with genes inferred to have been under selection in gray. The second row plots the relationship between estimates of the population recombination rate  $\rho$  in teosinte (x axis) versus maize (y axis) (14). Estimates of  $\rho$  were calculated using Hudson's (9) composite likelihood estimator. The third row shows a histogram of the frequency distribution of Tajima's  $D$  in maize (black) and teosinte (gray). The cumulative distribution of Tajima's  $D$  is also given.  $\Delta D$  is the difference in average  $D$  values between maize and teosinte.

lated data set under the ML estimate of  $\hat{k} = 2.45$  and compared simulated data to our observed data. The observed shifts in diversity ( $\theta$ ), frequency spectrum ( $D$ ), and recombination ( $\rho$ ) between teosinte and maize fit closely with simulated data (Fig. 1). However, the absolute values of  $D$  in simulated data do not fully agree with observed values, perhaps because of some feature of teosinte demographic history that is not fully captured by our model. Nonetheless, the most likely bottleneck model is generally consistent with observed patterns of sequence diversity.

Although there is a generally good fit of the bottleneck model, selection at some loci

can skew the distribution of polymorphism across loci. In particular,  $\sim 10\%$  of our loci have zero diversity in maize; it is unclear whether a domestication bottleneck alone can explain this observation. To examine this, we developed a likelihood ratio (LR) test to determine whether the entire data set is consistent with a single domestication bottleneck or whether the multilocus data are better explained by two classes of genes—one consisting of nonselected genes that have experienced the domestication bottleneck ( $k_1$ ), the other consisting of selected genes that have experienced a more severe bottleneck ( $k_2$ ) that mimics selection. Our method simul-

taneously estimates the severity of both bottlenecks ( $k_1$  and  $k_2$ ) and also estimates the proportion of genes ( $f$ ) that fit the severe bottleneck.

The LR test provides statistically significant support for the presence of two gene classes (LR = 5.8, df = 1,  $P < 0.05$ ). The first class has experienced a domestication bottleneck of severity  $\hat{k}_1 = 2.45$ , and the second class has undergone a bottleneck of more than 10 times the intensity ( $\hat{k}_2 = 0.15$ ). Under this model, the ML estimate of  $f$  is 0.02, indicating that 2% of our 774 maize genes are in the selected class. However, some of our 774 genes have low diversity in teosinte (Fig. 1). These genes provide little information to discriminate be-

**Table 1.** Candidate selected genes, sorted by posterior probability (PP).

Rank	Gene or locus	PP	Gene name or description	Putative gene function
	<i>tb1</i>	0.87	Teosinte branched 1 ( <i>tb1</i> )	Transcription factor
1	AY112154	0.77	Ribosomal protein L28 family	Structural constituent of ribosome
2	AY105809	0.65	Acetyl transferase	Transferase activity
3*	AY107228	0.64	Dihydrodipicolinate synthase (DHPS)	Lysine biosynthesis
4*	AY106600	0.61	Adenylosuccinate synthetase	Purine biosynthesis
5	AY104983	0.59	Heat shock protein (hsp70)	Chaperone activity; protein folding
6†	AY105958	0.58	Auxin-induced protein	Transcription factor; response to sucrose
7	AY111546	0.57	Unknown	Unknown
8†	AY108246	0.55	Growth factor	
9	AY104090	0.54	Transmembrane protein	
10	AY111438	0.54	Glycosyltransferase	Transferase activity; carbohydrate biosynthesis
11	AY110082	0.53	Heat shock protein	Chaperone activity; protein folding
12†	AY104948	0.49	Auxin response factor (ARF1)	Transcription factor
13	AY106970	0.48	Unknown	
14	AY112083	0.47	Minichromosome maintenance factor 5	DNA-dependent ATPase activity; DNA replication initiation
15	AY106111	0.46	Hexokinase 1 (HXK1)	ATP binding
16	AY108481	0.45	Unknown	
17	AY104147	0.44	F-box family protein	
18*	AY107907	0.43	Chorismate mutase (CM2)	Aromatic amino acid biosynthesis
19*	AY105062	0.43	Microsomal signal peptidase (SPC25)	Peptidase activity
20*	AY107903	0.43	Ubiquitin C-terminal hydrolase family protein	Ubiquitin-dependent protein catabolism
21	AY104037	0.41	Aconitate hydratase	Aconitate hydratase activity
22	AY107173	0.40	Unknown	
23	AY103840	0.39	Ubiquitin/transferase family protein	Trichome branching; DNA endoreduplication
24	AY108543	0.38	Early responsive to dehydration protein	
25†	AY104065	0.36	Cell elongation protein DWARF1	Steroid biosynthesis; cell elongation; response to light
26*	AY104439	0.33	Indole synthase	Indole biosynthesis
27	AY108187	0.31	Unknown	
28	AY106496	0.30	Unknown	
29	AY104530	0.28	CBL-interacting protein kinase 3 (CIPK3)	Kinase activity; response to abiotic stimulus
30	AY107475	0.27	Basic endochitinase	Chitinase activity; anti-fungal peptide activity

\*Genes with putative function in amino acid biosynthesis.

†Genes with putative function in plant growth.

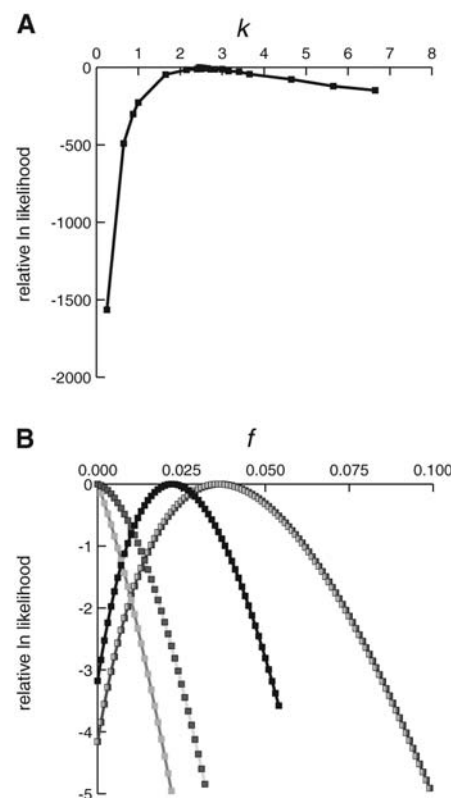


**Fig. 2.** Likelihood results fitting the population bottleneck. (A) Likelihood surface for the strength of the population bottleneck,  $k$ , based on all 774 loci. (B) The black points show the likelihood surface fitting  $f$ , the proportion of genes in the severe bottleneck (selected) class, using the most likely two-bottleneck model ( $k_1 = 0.15$ ,  $k_2 = 2.45$ ) and all 774 loci. The gray hatched curve to the right shows the likelihood surface fitting  $f$  using the most likely two-bottleneck model ( $k_1 = 0.001$ ,  $k_2 = 2.45$ ) and loci with 10 or more segregating sites in teosinte. The two curves on the left, both with an apex at  $f = 0.00$ , represent the likelihood surface for  $f$  based on analysis of data sets simulated with a single bottleneck using rejection sampling (14). The analysis correctly estimates  $f$  to be zero, as expected under neutrality. The light gray curve with apex at  $f = 0.00$  is based on a simulated data set from one bottleneck that is also conditioned on the observed frequency spectrum (Tajima's  $D$ ) in teosinte.

tween the two gene classes and therefore affect the estimation of  $f$ . When we conduct the LR test on 275 genes with relatively high polymorphism in teosinte (10 or more segregating sites), the proportion of genes under selection increases to  $\hat{f} = 3.6\%$  (LR = 4.6,  $P < 0.05$ ,  $\hat{k}_1 = 2.45$ ,  $\hat{k}_2 = 0.001$ ). Thus, our likelihood analysis estimates that 2 to 4% of maize genes have been selected during maize domestication and improvement. Note that nonzero estimates of  $f$  are not expected under a single, moderate population bottleneck, even when we account

fully for the skewed frequency distribution in teosinte (Fig. 2B).

Given these results, we used our likelihood framework to identify candidate selected genes by calculating the posterior probability (PP) that a gene is in the selected class (14). Table 1 shows the ranked PP for the top 4% of the candidate genes in our data set, as well as the PP for the *tb1* locus. *tb1* is included as a positive control because there is strong morphological and genetic evidence for selection on *tb1* during domestication (2, 17, 18). The

statistical power to detect selection may be higher for *tb1* than for most of our genes because the sequences are longer and the maize sample is larger. Nonetheless, our method correctly identifies *tb1* as a member of the selected class, with *tb1* assigned the highest PP (87%) among all genes.

The top candidate genes from our data set include genes known to be involved in plant growth and auxin response, which may contribute to the morphological differences between maize and teosinte (Table 1). In addition, our candidates identified a novel class of selected genes that function in amino acid biosynthesis and protein catabolism, suggesting selection for amino acid composition. Our inbred lines represent maize genetic diversity after domestication and breeding. We therefore cannot determine whether our high-PP genes were selected during the initial domestication event, during subsequent breeding and improvement, or both. However, amino acid composition is known to differ between maize and teosinte (19), and it is an important current target of selection for nutrition.

Previous studies (20, 21) have identified quantitative trait loci (QTLs) for phenotypic differences between maize and teosinte. We plotted the estimated map positions of these QTLs with the PP for each of the 638 mapped loci in our study (Fig. 3) (table S2). A number of high-PP genes map near QTLs, particularly on chromosomes 1 and 5, which suggests that we may have identified selected genes associated with these morphological differences. The average distance from estimated map positions of QTLs is significantly lower for the top 4% of the candidate genes than for the rest of our 638 loci (permutation test,  $P < 0.05$ ), and thus our selected genes cluster near QTLs. However, these QTLs contribute to morphological differences between species, and some of our candidates appear to be associated with other types of selection, such as biochemical composition, that we do not expect to be associated with the QTLs. Accordingly, growth-associated candidate genes and QTL locations remain clustered ( $P < 0.01$ ), but amino acid biosynthesis genes do not cluster with QTLs ( $P = 0.66$ ). The distribution of candidate genes also suggests that a number of selected genes fall under a single QTL (Fig. 3); this implies that morphological differentiation at a given QTL may be caused by a cluster of loci in the same pathway, consistent with a long-standing hypothesis for maize evolution (1).

We estimate that 2 to 4% of maize genes were selected during domestication and subsequent improvement. If we assume that our sample of genes is representative of the genome as a whole and that maize contains 59,000 genes (22), our results suggest that a minimum of  $59,000 \times 2\% \approx 1200$  genes throughout the genome have been targets of selection during

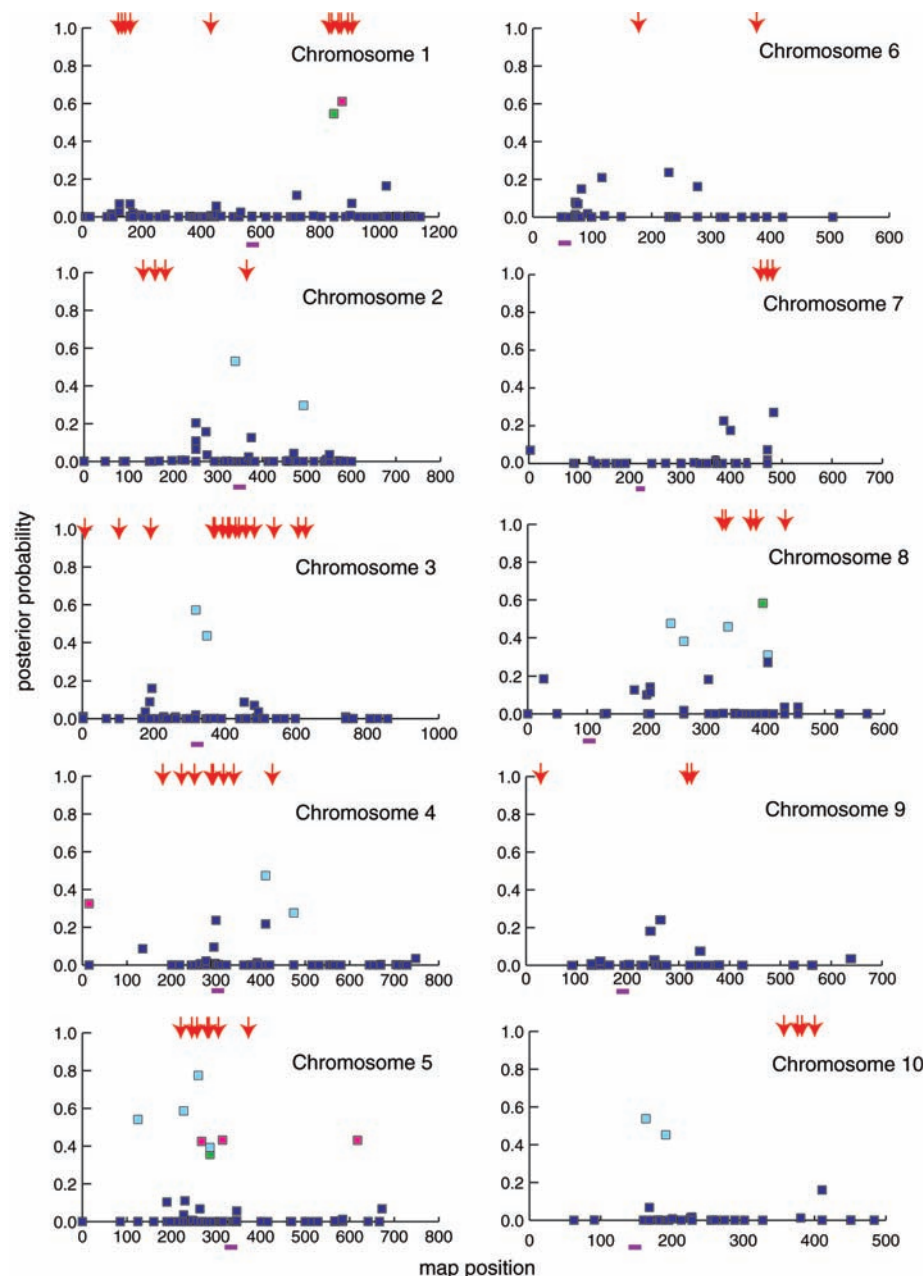


**Fig. 3.** Graphs of the posterior probabilities (PP) and map positions of 638 mapped genes (squares) against the estimated chromosomal locations of QTLs (red arrows) associated with a suite of morphological differences between teosinte and maize. Light blue, green, and magenta squares denote the top 30 high-PP genes listed in Table 1. Genes in green have a putative function in plant growth (genes 6, 8, 12, and 25 in Table 1). Genes in magenta putatively function in amino acid biosynthesis (genes 3, 4, 18, 19, 20, and 26 in Table 1). The centromeric position for each chromosome is identified by a purple line under the x axis. Chromosomal positions are roughly in units of 0.25 cM.

maize domestication and improvement. However, some of our candidate genes could be false positives, for three reasons. First, loci with very skewed frequency distributions in teosinte could lose more polymorphism during the domestication bottleneck than expected under our model, causing false inference of selection. Second, although our method confirms that the multilocus distribution of genetic diversity is inconsistent with a single bottleneck, any single gene could fall into the selected class by stochastic (nonselective) effects. Finally, rather than being the direct targets of selection, some loci could be hitchhiking with a site under selection. Indeed, candidate genes are significantly closer to the centromere than are non-candidates ( $P < 0.05$ ), which suggests a greater chance of detecting selection in regions of reduced recombination, where hitchhiking should be more pronounced (23). Nonetheless, previous studies have shown that hitchhiked regions in maize tend to be relatively short (2, 24), and recombination in maize coding regions is sufficient to severely limit the physical extent of hitchhiking to one, or at most a few (25), genes. Additionally, the subset of candidates for growth and amino acid biosynthesis are not significantly closer than noncandidate genes to the centromeres ( $P = 0.49$ ), which suggests that these candidates are direct targets of selection.

Despite these caveats, our estimate of 2 to 4% of genes having been under selection is likely conservative, for three reasons. First, if selection acted on moderate-frequency variants in teosinte, selection may have had little effect on diversity levels (4). In such cases, there is little power to detect selection. Second, our method assumes that selected genes are represented by a single severe bottleneck. This approach may not detect genes subjected to subtle selection regimes. Third, high recombination rates within maize genes could reduce the hitchhiking effect to the point that only short fragments within genes retain the footprint of selection. In *tb1*, for example, selection in the promoter region did not affect diversity in the coding region (2). It is thus possible that we sequenced a region within a bona fide selected gene, but our region did not retain evidence of selection.

Maize domestication prompted phenotypic change that is more extensive than in most domesticated plant species. It is thus possible that maize has a higher proportion of selected genes than most domesticates, but similar studies of additional domesticated species are required to address this issue. We have shown that our candidate genes are associated with QTL regions underlying phenotypic differences between maize and teosinte, which suggests that they contribute to traits selected during domestication. Note that these genes are depauperate for polymorphism in maize, and hence it is unlikely that they could have been

identified by methods that require segregating variation within maize, such as QTL or association analysis. The statistical methodology designed for this study will prove helpful both for identifying new candidates in maize and for application to other species, such as humans, where there is interest in selection on genes during the migration of modern humans out of Africa [e.g., (26)]. Finally, additional studies of our high-PP genes may provide important insight into the pathways and mutations responsible for maize evolution.

References and Notes

1. J. Doebley, *Annu. Rev. Genet.* **38**, 37 (2004).
2. R. L. Wang, A. Stec, J. Hey, L. Lukens, J. Doebley, *Nature* **398**, 236 (1999).
3. E. S. Buckler, J. M. Thornsberry, S. Kresovich, *Genet. Res.* **77**, 213 (2001).
4. H. Innan, Y. Kim, *Proc. Natl. Acad. Sci. U.S.A.* **101**, 10667 (2004).
5. N. Galtier, F. Depaulis, N. H. Barton, *Genetics* **155**, 981 (2000).
6. G. A. Watterson, *Theor. Popul. Biol.* **7**, 256 (1975).
7. M. I. Tenaillon, J. U'Ren, O. Tenaillon, B. S. Gaut, *Mol. Biol. Evol.* **21**, 1214 (2004).
8. L. Zhang, A. S. Peck, D. Dunams, B. S. Gaut, *Genetics* **162**, 851 (2002).
9. R. R. Hudson, *Genetics* **159**, 1805 (2001).
10. J. D. Wall, P. Andolfatto, M. Przeworski, *Genetics* **162**, 203 (2002).
11. F. Tajima, *Genetics* **123**, 597 (1989).
12. A. Eyre-Walker, R. L. Gaut, H. Hilton, D. L. Feldman, B. S. Gaut, *Proc. Natl. Acad. Sci. U.S.A.* **95**, 4441 (1998).

13. Y. Matsuoka et al., *Proc. Natl. Acad. Sci. U.S.A.* **99**, 6080 (2002).
14. See supporting data on Science Online.
15. H. Hilton, B. S. Gaut, *Genetics* **150**, 863 (1998).
16. Y. Vigouroux et al., *Mol. Biol. Evol.* **19**, 1251 (2002).
17. J. Doebley, A. Stec, C. Gustus, *Genetics* **141**, 333 (1995).
18. R. M. Clark, E. Linton, J. Messing, J. F. Doebley, *Proc. Natl. Acad. Sci. U.S.A.* **101**, 700 (2004).
19. R. Bressani, E. T. Mertz, *Cereal Chem.* **35**, 227 (1958).
20. J. Doebley, A. Stec, *Genetics* **134**, 559 (1993).
21. J. Doebley, A. Stec, *Genetics* **129**, 285 (1991).
22. J. Messing et al., *Proc. Natl. Acad. Sci. U.S.A.* **101**, 14349 (2004).
23. J. Maynard Smith, J. Haigh, *Genet. Res.* **23**, 23 (1974).
24. S. R. Whitt, L. M. Wilson, M. I. Tenaillon, B. S. Gaut, E. S. t. Buckler, *Proc. Natl. Acad. Sci. U.S.A.* **99**, 12959 (2002).
25. K. Palaisa, M. Morgante, S. Tingey, A. Rafalski, *Proc. Natl. Acad. Sci. U.S.A.* **101**, 9885 (2004).
26. J. M. Akey et al., *PLoS Biol.* **2**, e286 (2004).
27. We thank P. Morrell, M. Clegg, T. Long, S. McDonald, M. Przeworski, and P. Andolfatto for comments and discussion; K. Houchins, L. Schultz, and N. Duru for technical assistance; and S. Frank and L. Donaldson for use of computer clusters. Supported by NSF grants DBI0096033, DBI9872655, and DBI0321467 and by the USDA–Agricultural Research Service.

Supporting Online Material

www.sciencemag.org/cgi/content/full/308/5726/1310/DC1  
 Materials and Methods  
 Figs. S1 and S2  
 Tables S1 and S2  
 References

24 April 2005; accepted 9 May 2005  
 10.1126/science.1107891

# Resting Microglial Cells Are Highly Dynamic Surveillants of Brain Parenchyma in Vivo

Axel Nimmerjahn,<sup>1</sup> Frank Kirchhoff,<sup>2</sup> Fritjof Helmchen<sup>1\*</sup>

Microglial cells represent the immune system of the mammalian brain and therefore are critically involved in various injuries and diseases. Little is known about their role in the healthy brain and their immediate reaction to brain damage. By using in vivo two-photon imaging in neocortex, we found that microglial cells are highly active in their presumed resting state, continually surveying their microenvironment with extremely motile processes and protrusions. Furthermore, blood-brain barrier disruption provoked immediate and focal activation of microglia, switching their behavior from patrolling to shielding of the injured site. Microglia thus are busy and vigilant housekeepers in the adult brain.

Microglial cells are the primary immune effector cells in the brain. In response to any kind of brain damage or injury, microglial cells become activated and undergo morphological as well as functional transformations. They are critically involved in lesions, neurodegenerative diseases, stroke, and brain tumors

(1–4). Resident microglial cells in the healthy brain are thought to rest in a dormant state, whereas activation is associated with structural changes, such as motile branches or migration of somata (5, 6). However, because most tissue preparations represent traumatic injuries by themselves, key aspects of microglia function have remained elusive.

Here, we investigated microglia behavior in intact adult brains both during the resting state and immediately after local injury by using in vivo two-photon microscopy (7). We used transgenic mice showing specific expression of enhanced green fluorescent protein

<sup>1</sup>Abteilung Zellphysiologie, Max Planck Institut für Medizinische Forschung, Jahnstrasse 29, 69120 Heidelberg, Germany. <sup>2</sup>Abteilung Neurogenetik, Max Planck Institut für Experimentelle Medizin, Hermann-Rein-Strasse 3, 37075 Göttingen, Germany.

\*To whom correspondence should be addressed. E-mail: fritjof@mpimf-heidelberg.mpg.de

# ERRATUM

post date 7 October 2005

**Reports:** "The effects of artificial selection on the maize genome" by S. I. Wright *et al.* (27 May 2005, p. 1310). In the first full paragraph of the third column on p. 1312, the value of the likelihood ratio (LR) is incorrect. The sentence should read, "The LR provides statistically significant support for the presence of two gene classes (LR = 6.35, df = 2,  $P < 0.05$ )." This correction does not modify the results or the conclusions in any way. In addition, in the first column of p. 1313, the LR statistic should read, "(LR = 4.6, df = 2,  $P = 0.10$ ,  $\hat{k}_1 = 2.45$ ,  $\hat{k}_2 = 0.001$ )." With this correction, statistical support for the selection model with the reduced data set is borderline significant. However, the author's best estimate of  $f$  based on the reduced data remains 3.6%, and this correction does not substantially modify the results or the interpretation since statistical support for selection was obtained from the full data set.